Temperature dependence of planar channeling radiation in silicon, germanium, and beryllium between 12 and 330 K

G. Buschhorn, E. Diedrich, W. Kufner, and M. Rzepka
Max-Planck-Institut für Physik, D-80805 München, Germany

H. Genz, P. Hoffmann-Stascheck, and A. Richter
Institut für Kernphysik, Technische Hochschule Darmstadt, D-64289 Darmstadt, Germany
(Received 17 June 1996; revised manuscript received 27 September 1996)

The temperature dependence of planar channeling radiation of 62.8 MeV electrons has been studied for silicon, germanium, and beryllium. The measurements have been performed using an uncollimated low-emittance cw beam from the superconducting electron linac S-DALINAC at the Technische Hochschule Darmstadt. Energies and linewidths of transitions between transverse bound states have been determined in the energy range between 40 and 230 keV for silicon and beryllium at temperatures between 12 and 330 K, and for germanium between 12 and 223 K. From the shift of the transition energies with temperature the mean thermal vibrational amplitudes of the atoms transverse to the channeling planes are determined by comparison with calculations using the many-beam formalism. Within experimental errors no directional dependence of the vibrations is observed. For silicon a Debye temperature of (535.2 ± 8.5) K at 12 K and (519.0 ± 10.8) K at 300 K has been derived. For germanium an increase from (232.7 ± 12.8) K at 12 K to (292.0 ± 16.4) K at 223 K is observed. Planar channeling radiation spectra from a beryllium crystal taken at 12, 220, and 300 K have been analyzed the same way yielding a Debye temperature of (1060 ± 50) K. [S0163-1829(97)03110-X]

I. INTRODUCTION

Channeling radiation is produced when a beam of relativistic charged particles traverses a crystal under a sufficiently small angle with respect to a prominent crystal plane or axis. As demonstrated in a classic approach by Lindhard[1] the motion of the particles under these conditions is no longer determined by independent single atomic scattering processes but is dominated by correlated scattering on very many atoms along the path of the particle. Some particles are bound by the transverse potential of the crystal and channel through the crystal along the particular plane or axis. Classically, these particles describe a periodic transverse motion in the crystal potential resulting for light particles (electrons and positrons) in the emission of electromagnetic dipole radiation. For relativistic particles the dipole radiation is Lorentz-boosted leading in the laboratory frame to radiation in the forward direction at higher frequencies. Quantum mechanically the radiation is due to spontaneous transitions between transverse energy states of the electron resulting in discrete photon lines. The density of the energy states depends on the energy and the charge of the particle as well as on the crystal properties. Most studies of the properties of channeling radiation and its applications have been performed with electrons which channel in the neighborhood of the positively charged atomic nuclei. A review of experimental results and theoretical treatments of channeling radiation can be found in Ref. 2.

Channeling radiation, besides being of interest in its own, can be used as a tool in solid state physics to study crystal properties. In this paper we investigate the temperature dependence of the photon lines corresponding to transitions between low lying bound states which by comparison with calculated spectra can be used to determine the mean thermal atomic vibrational amplitudes transverse to the particular lattice plane. From these amplitudes the Debye temperature of the crystal can be derived. Although the results will be stated in terms of Debye temperatures, the theory applied does not use a Debye model for lattice vibrations.

The paper is organized as follows. Sections II and III give a brief description of the theoretical concepts and our experimental setup, respectively. In Sec. IV we present our methods of analyzing the data, in particular the treatment of multiple scattering of the electrons in the crystal and our results on vibrational amplitudes and Debye temperatures. In addition, we give the line widths of the channeling radiation lines which depend strongly on temperature. In the last section we discuss our results and compare with Debye temperatures derived by x-ray scattering and specific-heat measurements.

II. THEORETICAL CONCEPTS

Channeling radiation from relativistic electrons in single crystals has been studied for a number of years and is now a well understood phenomenon. We summarize here briefly the ''many-beam formalism'' introduced by Andersen *et al.*[3] for the calculation of the transition energies of planar channeling radiation.

Under channeling conditions the longitudinal and transverse motion of the electrons in the crystal can be separated. In first order the transverse motion is determined by the one-dimensional continuum potential $U(x)$ given by the average of the crystal potential $U(\mathbf{r},t)$ along the coordinates parallel to the plane.[1] This is equivalent to averaging over time, i.e., over thermal lattice vibrations, since different crystal atoms oscillate independently. Higher order effects and the treatment of periodic perturbations are discussed quantitatively by Hau and Andersen.[4] The resulting corrections to transition

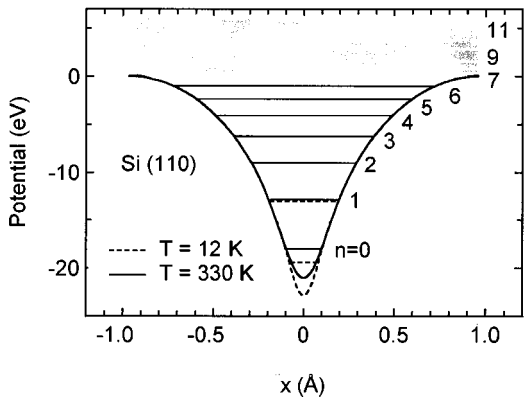

FIG. 1. Continuum potential of the Si(110) plane for $T=12$ K and $T=330$ K. In addition, the transverse eigenstates are given for 62.8 MeV electrons. The quasifree eigenstates above the potential maximum are smeared out to energy bands due to Bloch-wave broadening. As indicated, only the two lowest lying states ($n=0,1$) depend significantly on temperature.

line energies of the order 10^{-3} or less are within our experimental error and are therefore neglected. The periodic continuum potential $U(x)=\Sigma_n e^{ingx}U_n$ is expressed in terms of the Fourier components

$$U_n=\frac{2\pi\hbar^2}{meV_E}\sum_j e^{-ingx_j}A_j(ng)e^{-1/2(ng)^2\rho^2} \tag{1}$$

with A_j being the atomic scattering amplitude, g the reciprocal lattice vector, V_E the volume of the unit cell, x_j the relative positions of the j atoms in the unit cell, and ρ the rms thermal vibrational amplitude in one dimension. For our calculations we used tabulated values of A_j derived from Hartree-Fock calculations.[5]

Figure 1 shows the potential calculated according to Eq. (1) for the Si(110) plane for two different values of ρ corresponding to temperatures of 12 and 330 K, respectively. The minimum of the potential near the crystal atoms depends strongly on temperature due to different ''smearing'' of the atomic Coulomb potential by thermal vibrations.

The electron wave function $\Psi(x)$ in the transverse continuum potential $U(x)$ is given by

$$\left[-\frac{\hbar^2}{2\gamma m}\frac{\partial}{\partial x^2}+U(x)\right]\Psi(x)=E_\perp\Psi(x) \tag{2}$$

with $E_\perp$ denoting the transverse energy states, $\gamma=E/m$ and E the (total) electron energy. Figure 1 also shows the energy levels calculated according to Eqs. (1) and (2) for 62.8 MeV electrons channeling along the (110) plane in silicon.

The energy states can be classified into three groups: (i) States near and above the potential maximum are forming energy bands due to Bloch-wave broadening. As a consequence, transitions involving these states do not show up as sharp lines in the photon spectrum. (ii) States near the potential minimum ($n=0$, $n=1$), which significantly depend on the lattice vibrational amplitude (and therefore on temperature). Transitions to these states, in particular to the lowest lying state $n=0$ with even parity, will lead to increasing line energies with falling temperature. (iii) Intermediate states; transitions between these states have sharp energies, independent of temperature. They can be used in the analysis to determine the exact electron energy and the amount of multiple scattering.

In the laboratory frame the measured transition energies are Lorentz-boosted and given by

$$E_{nm}=\frac{2\gamma^2}{1+\gamma^2\Theta^2}(E_n-E_m) \tag{3}$$

with Θ being the angle between the electron and the radiated photon originating from multiple scattering, beam divergence, and detector aperture (see Sec. IV). Therefore, the average measured photon energy is less than $2\gamma^2(E_n-E_m)$.

III. EXPERIMENT

A. Electron beam and channeling setup

The experiment was carried out at the superconducting Darmstadt electron linear accelerator S-DALINAC.[6] An uncollimated cw beam of (62.8 ± 0.3) MeV electrons has been steered onto the crystal mounted on a goniometer situated inside a vacuum chamber. The beam current was of the order of 1 nA. The beam spot size, position, direction, and divergence were measured and monitored by means of two retractable fluorescence screens positioned 5.4 m apart upstream and downstream the channeling crystal. The beam was focussed to a diameter of 2 to 3 mm and a divergence of less than 0.6 mrad which is smaller than the critical channeling angle[1] typical for the conditions of this experiment ($\varphi_c=0.8$ mrad). After leaving the crystal the electrons were deflected by a 40° bending magnet.

The radiation produced by the channeling process in the crystal has been detected in the forward direction about 9 m downstream from the crystal by means of a germanium detector of 15-mm thickness and 16-mm diameter. The acceptance of the photon detector was limited to 1.2×10^{-6} sr by means of a cylindrical lead collimator (aperture 0.6 mrad) aligned with the direction of the undeflected electron beam within 0.2 mrad.[7]

B. Goniometer, crystals, and crystal cooling

For the investigation of the temperature dependence of the channeling spectra the crystal temperature has to be varied between 10 K and room temperature. This required to decouple the crystal thermally as much as possible from the goniometer which itself had to be kept at room temperature.

The scattering chamber containing the crystal is shown schematically in Fig. 2(a). A commercial helium bath cryostat was modified such that the vacuum of the scattering chamber (typically 10^{-5} Torr) served as insulation vacuum of the cryostat. The cooling tip of the cryostat was connected via a flexible copper cord of 30 mm^2 cross section with the crystal holder also made of copper. The crystal holder was mounted on a piece of rohacell connected to the goniometer. The cooling tip, the cooper cord, and the crystal holder were protected against thermal radiation by means of a superinsu-

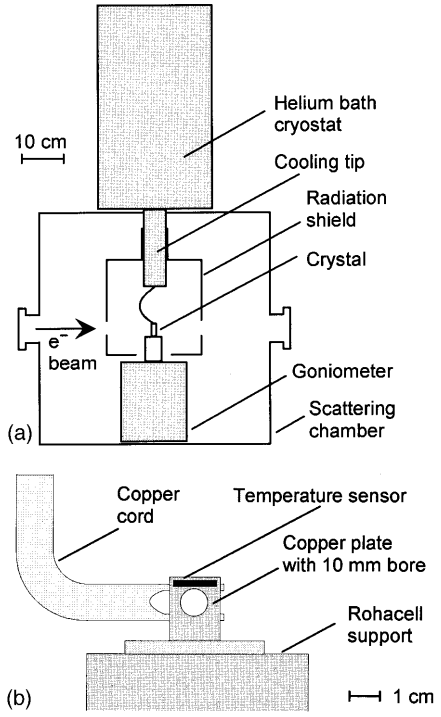

FIG. 2. (a) Schematic view of the scattering chamber with cryostat, goniometer, radiation shield, and crystal. The crystal holder was cooled by means of a thick copper cable connected to a helium dewar. (b) Detailed view of the crystal holder. The crystal covers the 10-mm bore of a copper plate and is attached and thermally connected on this plate by means of heat conducting grease. The temperature of the copper plate is measured by a platinum resistivity temperature sensor thermally connected to the plate.

lation shield (20 layers of aluminized Mylarfoil) provided with openings for nonobstructed passage of the electron beam.

The crystal holder [Fig. 2(b)] consisted of a copper plate of 1-mm thickness with a bore of 10 mm. The crystal (typical size 12×12 mm^2) were fixed to the holder by means of heat conducting vacuum grease. Three crystals were used in the experiment: silicon ($Z=14$) and germanium ($Z=32$) crystals, both 50-μm thick and cut perpendicular to the $\langle100\rangle$ axis, and a 100-μm-thick beryllium crystal ($Z=4$) cut perpendicular to the $\langle00.1\rangle$ axis.

The temperature of the crystal holder was measured using a platinum resistor sensor mounted directly onto the copper plate [Fig. 2(b)]. The maximum temperature difference between the copper plate and the center of the crystal is estimated to less than 0.1 K for all crystals. The lowest crystal temperature achieved in the experiment was 12 K. Higher temperatures could be adjusted by heating the cooling tip and changing the helium flow through the cryostat with a temperature stability measured at the crystal holder of better than 0.5 K.

The crystal could be oriented by means of a two-axis goniometer (one horizontal, one vertical axis) with an angular resolution of 0.175 mrad which is less than the critical angle of 0.8 mrad. Two additional translational stages enabled to move the cooled crystal into and out of the beam for alignment and background studies.

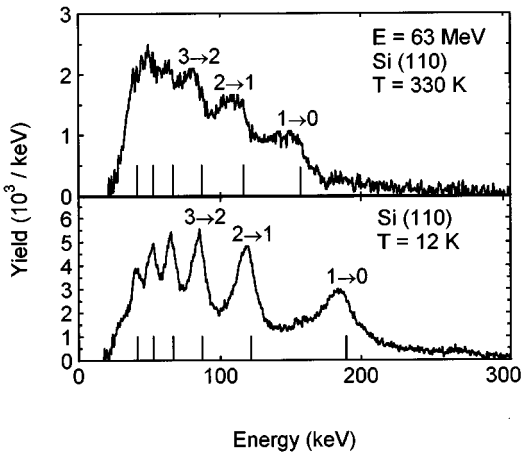

FIG. 3. Channeling spectra of the Si(110) plane for $T=330$ K and $T=12$ K. In these spectra both the incoherent bremsstrahlung background and the continuum contribution of channeling radiation due to free-to-free (or free-to-bound) transitions are substracted; the spectra are not normalized to each other. The vertical lines indicate the calculated transition energies for an ideal thin crystal [see Eq. (3) with $\Theta=0$]. The maxima of the measured lines are shifted to lower energies mainly due to multiple scattering in the crystal (see text).

IV. RESULTS

A. Data analysis

Channeling radiation can be classified in terms of bound-bound, free-bound, and free-free transitions depending on the involved eigenstates. For the electron energy and crystals used in this experiment there exist only a few allowed bound-bound transitions leading to well separated channeling lines in the photon energy spectrum which can be used for the analysis. The numerous transitions starting at free levels (free-bound and free-free) sum up to a broad continuum which amounts to about 10–20% of the integral channeling intensity depending on the crystal plane. The shape of this background and thus its contribution to the discrete lines can be calculated by the many-beam formalism and is independent of temperature. An additional background contribution is caused by incoherent bremsstrahlung which has been measured independently with the crystal in a random orientation. These two background contributions have been normalized and subtracted in such a way, that the resulting bound-bound channeling spectra vanish in the energy regions below (<20 keV) and above (>300 keV) the channeling lines. A detailed description of the background subtraction procedure is given in Ref. 8. As an example, the resulting channeling line spectra of the Si(110) plane are shown for $T=330$ and 12 K in Fig. 3.

The natural width Γ_0 of the photon lines is related to the lifetimes of the involved channeling states limited by (among other sources[9]) incoherent scattering at crystal atoms and electrons. For a discussion on how to relate Γ_0 to the decay constant of the state involved in the transition we refer to Ref. 4. The quantity Γ_0 is not directly measured in the experiment but has to be deduced from the measured line width

which receives contributions from the energy resolution of the detector, finite crystal thickness, multiple scattering of the electrons in the crystal, the beam divergence, and the detector aperture. The detector resolution Γ_D is 1.0 to 1.5 keV full width at half maximum in the energy range of interest and adds quadratically to Γ_0. The contribution due to the finite crystal thickness L is given by $(1+\beta)\gamma^2 2\pi\hbar c/L$,[14] which yields 0.76 eV for the used silicon and germanium crystals and 0.38 eV for the beryllium crystal. These small values also add approximately quadratically to Γ_0. The other effects mentioned concern the angle Θ between the electron and the photon observational direction. Increasing Θ decreases the measured photon energy according to Eq. (3) resulting in a downward shift of the energy of the channeling radiation line as compared to $\Theta=0°$ and an asymmetric line shape as can be seen in Fig. 3.

With respect to multiple scattering one has to distinguish between scattering parallel and transverse to the channeling plane. The latter causes a redistribution of the channeling population densities $f_n(i)$ and dechanneling of the electrons. This effect thus determines the lifetime of the transverse bound states and therefore the intrinsic line width Γ_0. In contrast, multiple scattering parallel to the channeling plane only changes the angle Θ between the electron and the photon observational direction and thus the observed photon energy. The resulting mean scattering angle suffered by an electron of momentum p after traversing a crystal thickness z is given by[10]

$$\Theta_s(z)=\frac{E_S}{\sqrt{2}pc\beta}\sqrt{\frac{z}{X_0}} \tag{4}$$

with X_0 being the radiation length ($X_0=9.36$, 2.30, and 35.3 cm for Si, Ge, and Be, respectively). The energy constant E_S decreases logarithmically with decreasing z/X_0. For the calculations we have used $E_S=12$ MeV, which is accurate to 20% for all crystals used in the experiment.[10]

The mean scattering angle Θ_s for a given crystal and crystal thickness is given by the average of $\Theta_s(z)$ over the crystal thickness d weighted by the depth dependent channeling population density $f(z)$ which is assumed to decrease exponentially[11,12] with a characteristic length (''occupation length'') for 62.8 MeV electrons of 35, 17, and 67 μm for silicon, germanium, and beryllium, respectively. The value for silicon is a linear extrapolation of the measurement of Ref. 11 for 17 and 54 MeV electrons. These measurements show that the occupation length is nearly independent of the channeling state with possibly a small dependence on the channeling plane. For our estimate of the scattering angle we use an average of the measured occupation lengths for the (100) and (110) planes. The values for germanium and beryllium are obtained by scaling the silicon value with $\sqrt{X_0}$. Multiple scattering, detector aperture, and beam divergence combine to a mean square angle Θ between electron and photon given by $\Theta^2=\Theta_s^2+\Theta_a^2+\Theta_d^2$. As described in Sec. III the detector aperture was $\Theta_a=0.6$ mrad and the beam divergence approximately $\Theta_d=0.6$ mrad. This leads to $\Theta=2.0\pm0.3$, 3.1 ± 0.6, and 1.6 ± 0.2 mrad for the silicon, germanium, and beryllium crystals, respectively.

The experimental line shape is given by

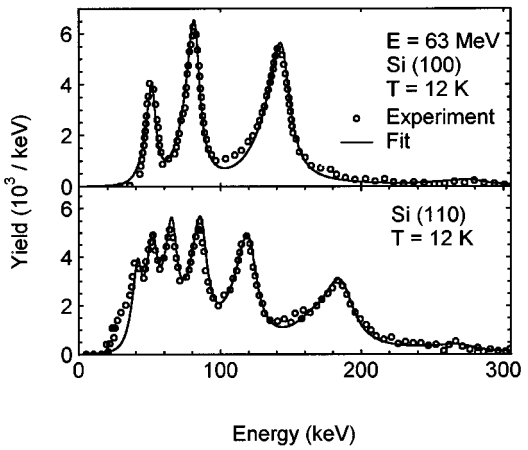

FIG. 4. Comparison of the measured spectra for the Si(100) and Si(110) planes (dots) with the result of a fit consisting of single ''Lorentz-shape'' transition lines asymmetrically broadened due to multiple scattering, beam divergence, and detector aperture according to Eq. (5). The experimental error is of the order of the symbol size.

$$I(E)\sim\int d\Theta\,\frac{E\Gamma}{[E-E_0(1+\Theta^2\gamma^2)^{-1}]^2+(1/4)\Gamma^2}\times\exp\left(-\frac{\Theta^2}{2\overline{\Theta}^2}\right), \tag{5}$$

where $\Gamma^2=\Gamma_0^2+\Gamma_D^2+\Gamma_T^2$, Γ_D being the energy resolution of the photon detector, Γ_T the finite thickness correction, and E_0 the transition energy. The mean emission angle Θ is assumed to be constant for a given crystal (neglecting small differences of the multiple scattering contribution for different crystal planes) and is determined by fitting Eq. (5) to the measured photon lines. This yields $\Theta=(2.1\pm0.2)$ and (3.7 ± 0.4) mrad for Si and Ge, respectively, which is consistent with the above estimated values. For beryllium the extracted value $\Theta=(3.8\pm0.6)$ mrad exceeds the calculated one of 1.6 mrad; this discrepancy is attributed to a mosaic spread as observed in a Laue diffraction analysis of the crystal which gives an additional contribution to Θ.

B. Thermal vibrational amplitudes and Debye temperature

Channeling radiation spectra for silicon and germanium have been measured for different temperatures starting at 12 K in steps of about 20 K up to 330 K for silicon and 223 K for germanium. A series of convoluted Lorentzians (5) has been fitted to each spectrum to extract intensity, energy E_0, and intrinsic line width Γ_0 for each transition line separately. As an example, Fig. 4 shows the comparison between measurements for the Si(100) and Si(110) planes at $T=12$ K and best fits. The corresponding line energies are shown in Fig. 5 for the Si(100) and Si(110) planes and the Ge(100) and Ge(310) planes as a function of temperature. To reproduce the experimental line energies many-beam calculations have been performed according to Eqs. (1)–(3). In the first step the energies of transitions between ''intermediate states'' (Sec. II), which do not depend on temperature, have been used to calibrate the electron energy separately yielding (62.8 ± 0.3) MeV. Then the experimental $1\rightarrow0$ transition en-

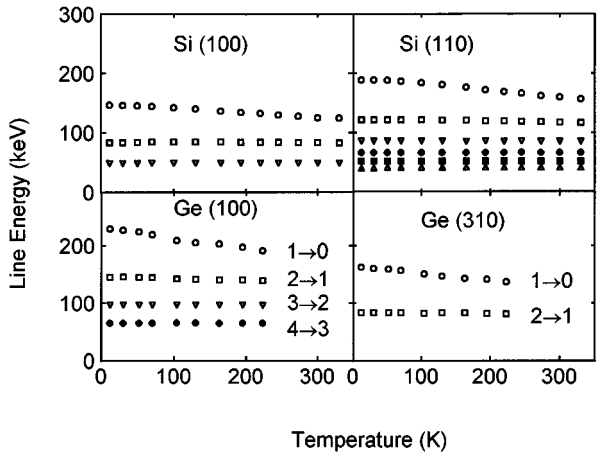

FIG. 5. Fitted line energies of $\Delta n=1$ transitions for the (100) and (110) planes for silicon and the (100) and (310) planes for germanium. As expected, only the $1\rightarrow0$ and (to a lesser extent) the $2\rightarrow1$ transition energies depend on temperature. The typical experimental errors are 0.6 keV for silicon and 2.6 keV for germanium given by the systematic error introduced by the background subtraction and the uncertainty in determining Θ.

ergies have been fitted with the mean square vibrational amplitude ρ^2 as a fit parameter for each plane and crystal temperature. Figure 6 shows the resulting temperature dependence of the thermal vibrational amplitude ρ. The experimental error (caused by the uncertainties in the experimental line energies and the electron energy) is of the order of the symbol size. Comparison of the data for different planes of the same crystal does not show significant differences. Thus, the thermal vibrational amplitude does not show any directional dependence.

In the Debye model the thermal vibrational amplitude ρ is related to the crystal temperature T according to[13]

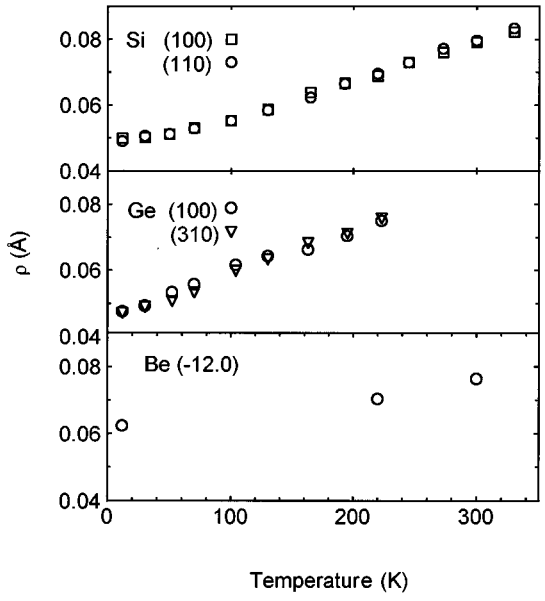

FIG. 6. Thermal vibrational amplitude for silicon, germanium, and beryllium as a function of temperature calculated from the transition line energies given in Fig. 5 using the many-beam formalism.

TABLE I. Experimentally determined Debye temperatures of silicon, germanium, and beryllium.

T [K]	Silicon Θ_D [K]	Germanium Θ_D [K]	Beryllium Θ_D [K]
12	535.2±8.5	232.7±12.8	1055±50
30	531.3±8.0	232.3±12.8	
50	533.4±8.3		
52		243.4±13.4	
70	529.9±8.3	254.1±12.4	
100	529.6±8.3		
104		259.8±14.2	
130	529.0±11.0	267.4±16.2	
163		282.6±16.4	
165	524.5±12.2		
193	522.3±10.8		
195		290.8±15.6	
220	526.1±11.5		1065±50
223		292.0±16.4	
245	552.2±10.0		
273	518.7±11.5		
300	519.0±10.8		1060±50
330	520.8±10.8		

$$\rho^2=\frac{3\hbar^2}{4Mk_B\Theta_D}\left[1+4\left(\frac{T}{\Theta_D}\right)^2\int_0^{\Theta_D/T}\frac{y}{\exp(y)-1}dy\right], \quad (6)$$

where Θ_D is the Debye temperature. Table I contains the values of the Debye temperature for silicon and germanium calculated from the ρ^2 data of these measurements.

For beryllium we have measured spectra at $T=12$, 220, and 300 K. As an example, Fig. 7 shows the radiation spectrum and the best fit at $T=12$ K for the (-12.0) plane. The resulting thermal vibrational amplitudes are shown in Fig. 6 corresponding to an approximately constant Debye temperature of $\Theta_D=(1060\pm50)$ K (see Table I).

C. Line widths

Figure 8 shows the intrinsic linewidth Γ_0 for the (100) and (110) planes in silicon and the (100) and (310) planes in germanium. As mentioned above, $1/\Gamma_0$ is proportional to the lifetime of the channeling states limited by incoherent scattering at crystal electrons and the nonperiodic part of the atomic potential, i.e., lattice defects and thermal vibrations.[4,9] Only thermal scattering depends on temperature leading to the observed increase of the linewidths of all measured channeling radiation lines with temperature. Neglecting contributions from scattering at crystal electrons, we have calculated the linewidth due to thermal atomic scattering following the

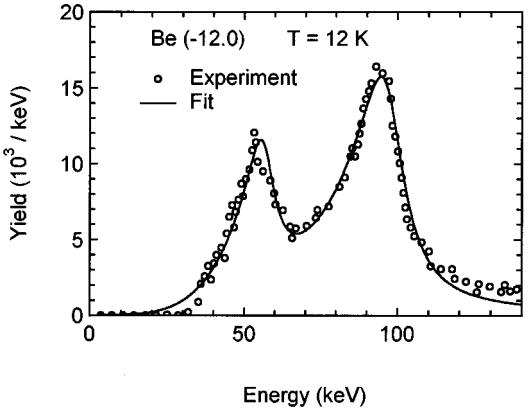

FIG. 7. Comparison of the measured spectrum for the (-12.0) plane in beryllium with the calculated spectrum for a Debye temperature $\Theta_D = 1060$ K which yields the best fit to the measured spectrum.

formalism given by Andersen *et al.*[14] There the linewidth is determined by the sum of the total probabilities for scattering from the initial or final states to any other state (interband scattering), corrected for scattering within each channeling state (intraband scattering). The curves in Fig. 8 show the results for germanium, which, in general, agree well with the measurements. In contrast, for silicon the calculated linewidths for all channeling transitions are lower than the measured ones by about 3 keV at all temperatures suggesting the existence of additional temperature independent contributions such as scattering on crystal imperfections or electronic scattering. As electronic scattering scales with Z and atomic scattering with Z^2, electronic scattering should be more important for silicon ($Z=14$) as for germanium ($Z=32$) in accordance with the measurement.

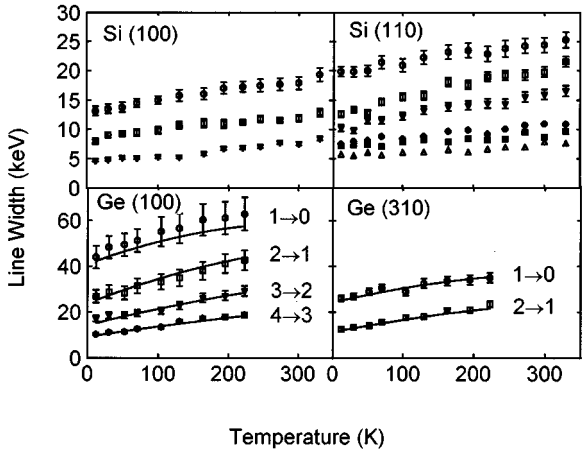

FIG. 8. Linewidth of the channeling radiation lines for the silicon (100) and (110) planes and the germanium (100) and (310) planes as a function of temperature. Plotted is the ''intrinsic'' linewidth corresponding to the lifetime of the bound states due to incoherent scattering of the electrons. The additional experimental contributions due to multiple scattering, beam divergence, nonvanishing detector aperture, and energy resolution have been deconvoluted from the measured linewidths.

V. SUMMARY AND CONCLUSIONS

We have investigated energy spectra of planar channeling radiation in silicon, germanium, and beryllium over a wide temperature range between 12 and 330 K and extracted the vibrational amplitudes ρ by comparison with many-beam calculations. Within experimental errors no directional dependence of the vibrations is observed. From the measurements of vibrational amplitudes we have deduced Debye temperatures for silicon, germanium, and beryllium at all temperatures covered in this experiment (see Table I).

For silicon at room temperature we deduce a vibrational amplitude $\rho=(0.0790\pm0.0005)$ Å, which corresponds to a Debye temperature of (519.0 ± 10.8) K. These values are consistent with other channeling radiation experiments, e.g., Kephart *et al.*,[15] who derived a mean value $\rho=(0.0796\pm0.0015)$ Å for an electron energy of 54.5 MeV and Hau *et al.*,[16] who obtained $\Theta_D=(504\pm6)$ K. All channeling experiments yield substantially lower values for the Debye temperature than those derived from x-ray scattering at lower order reflections [(543 ± 8) K in Ref. 17, (533 ± 2) K in Ref. 18] and neutron scattering [(538 ± 8) K in Ref. 19], which in turn are lower by about 20% than those calculated from specific-heat measurements.[20] On the other hand, high-precision measurements[21] of electronic charge distribution in silicon based on very high order x-ray diffraction are interpreted by the authors in terms of significantly lower Debye temperatures than those derived by Ref. 18 from lower order diffraction data. The high order diffraction is dominated by scattering off K shell electrons whereas lower order reflections receive contributions from all electrons. The combined x-ray data for Si thus hints to larger vibrational amplitudes of the core of lattice atoms as compared to the outer shell electrons. This is at least in qualitative accord with the channeling radiation results derived from transitions to the lowest lying transverse bound states which are localized near the atomic nuclei. For further discussions we refer to Ref. 16.

The measured Debye temperature of germanium rises significantly from (233 ± 13) K at 12 K to (292 ± 16) K at 223 K. For higher temperatures single radiation lines cannot be resolved in the germanium spectra. At room temperature x-ray scattering yields a Debye temperature of $\Theta_D=(290\pm5)$ K (Ref. 17) consistent with our measurements at 223 K.

For beryllium we determined a Debye temperature of $\Theta_D=(1060\pm50)$ K consistent in magnitude with the specific heat measurements of Hill and Smith[22] in the temperature range between 5 K ($\Theta_D=1160$ K) and 300 K ($\Theta_D=930$ K). But in contrast to Ref. 22, we do not see a significant temperature dependence of Θ_D.

ACKNOWLEDGMENTS

This work was supported by the German Federal Minister for Research and Technology (BMBF) under Contract No. 06DA665I. The authors wish to thank the technical staff of the Max-Planck-Institut für Physik, in particular W. Erbe, for their contributions to the construction and installation of the experiment and H.-D. Gräf and the S-DALINAC group for the excellent electron beams. The MPI authors gratefully acknowledge the hospitality extended to them at the Institut für Kernphysik at Darmstadt.

[1] J. Lindhard, K. Dan. Vidensk. Selsk. Mat. Fys. Medd. **34**, No. 14 (1965).
[2] *Coherent Radiation Sources*, edited by A. W. Sáenz and W. Überall (Springer, Berlin, 1985).
[3] J. U. Andersen, E. Bonderup, E. Laegsgaard, B. B. Marsh, and A. H. Sørensen, Nucl. Instrum. Methods Phys. Res. **194**, 209 (1982).
[4] L. V. Hau and J. U. Andersen, Phys. Rev. A **47**, 4007 (1993).
[5] P. A. Doyle and P. S. Turner, Acta Crystallogr. Sec. A **24**, 390 (1968).
[6] J. Auerhammer, H. Genz, H.-D. Gräf, R. Hahn, P. Hoffmann-Stascheck, C. Lüttge, U. Nething, K. Rühl, A. Richter, T. Rietdorf, P. Schardt, E. Spamer, F. Thomas, O. Titze, J. Töpper, and H. Weise, Nucl. Phys. A **553**, 841c (1993).
[7] M. Rzepka, G. Buschhorn, E. Diedrich, R. Kotthaus, W. Kufner, W. Rössl, K. H. Schmidt, P. Hoffmann-Stascheck, H. Genz, U. Nething, and A. Richter, Phys. Rev. B **52**, 771 (1995).
[8] W. Kufner, Ph.D. thesis, Technische Universität München, 1994.
[9] H. Genz, L. Groening, P. Hoffmann-Stascheck, A. Richter, M. Höfer, J. Hormes, U. Nething, J. P. F. Sellschop, C. Toepffer, and M. Weber, Phys. Rev. B **53**, 8922 (1996).
[10] V. L. Highland, Nucl. Instrum Methods **129**, 497 (1975).
[11] J. O. Kephart, R. H. Pantell, B. L. Berman, S. Datz, H. Park, and R. K. Klein, Phys. Rev. B **40**, 4249 (1989).
[12] U. Nething, M. Galemann, H. Genz, M. Höfer, P. Hoffmann-Stascheck, J. Hormes, A. Richter, and J. P. F. Sellschop, Phys. Rev. Lett. **72**, 2411 (1994).
[13] D. Gemmel, Rev. Mod. Phys. **46**, 129 (1974).
[14] J. U. Andersen, E. Bonderup, E. Laegsgaard, and A. H. Sørensen, Phys. Scripta **28**, 308 (1983).
[15] J. O. Kephart, B. L. Berman, R. H. Pantell, S. Datz, R. K. Klein, and H. Park, Phys. Rev. B **44**, 1992 (1991).
[16] L. V. Hau, E. Laegsgaard, and J. U. Andersen, Nucl. Instrum. Methods Phys. Res. B **48**, 244 (1990).
[17] B. W. Batterman and D. R. Chipman, Phys. Rev. **127**, 690 (1962).
[18] P. J. E. Aldred and M. Hart, Proc. R. Soc. London **A332**, 223 (1973).
[19] H. A. Graf, J. R. Schneider, A. K. Freund, and M. S. Lehmann, Acta Crystallogr. Sec. A **37**, 863 (1981).
[20] P. Flubacher, A. J. Leadbetter, and J. A. Morrison, Philos. Mag. **4**, 273 (1959).
[21] M. Deutsch and M. Hart, Phys. Rev. B **31**, 3846 (1985).
[22] R. W. Hill and P. L. Smith, Philos. Mag. **44**, 636 (1953).